Drainage, sediment transport, and denudation rates on the Nanga Parbat Himalaya, Pakistan

Kevin Cornwell[a,*], Doug Norsby[b], Richard Marston[c]

[a] Department of Geology, California State University-Sacramento, Sacramento, CA 95819-6043, USA
[b] Department of Public Works, Watershed Division, Topeka, KS 66215, USA
[c] School of Geology, Oklahoma State University, Stillwater, OK 74078, USA

Abstract

The Nanga Parbat Himalaya presents some of the greatest relief on Earth, yet sediment production and denudation rates have only been sporadically addressed. We utilized field measurements and computer models to estimate bank full discharge, sediment transport, and denudation rates for the Raikot and Buldar drainage basins (north slope of Nanga Parbat) and the upper reach of the Rupal drainage basin (south slope).

The overall tasks of determining stream flow conditions in such a dynamic geomorphic setting is challenging. No gage data exist for these drainage basins, and the overall character of the drainage basins (high relief, steep flow gradients, and turbulent flow conditions) does not lend itself to either ready access or complete profiling.

Cross-sectional profiles were surveyed through selected reaches of these drainage basins. These data were then incorporated into software (WinXSPRO) that aids in the characterization (stage, discharge, velocity, and shear stress) of high altitude, steep mountain stream conditions.

Complete field measurements of channel depths were rarely possible (except at several bridges where the middle of the channel could actually be straddled and probed) and, when coupled with velocity measurements, provided discrete points of field-measured discharge calculations. These points were then used to calibrate WinXSPRO results for the same reach and provided a confidence level for computer-generated results.

Flow calculations suggest that under near bank full conditions, the upper Raikot drainage basin produces discharges of ~ 61 cm and moves about 11,000 tons day^{-1} (9980 tons day^{-1}) of sediment through its channel. Bank full conditions on the upper portion of the Rupal drainage basin generate discharges of ~ 84 cm and moves only about 3800 tons day^{-1} (3450 tons day^{-1}) of sediment. Although the upper Rupal drainage basin moves more water, the lower slope of the drainage basin (0.03) generates a much smaller shear stress (461 Pa) than does the higher slope (0.12) of the upper Raikot drainage basin (1925 Pa).

Dissolved and suspended sediment loads were measured from water/sediment samples collected throughout the day and night over a period of 10 days at the height of the summer melt season but proved to be a minor variable in transport flux. Channel bed loads were measured using a pebble count method of bank material and then used to generate ratings curves of bed loads relative to discharge volumes. When coupled with discharge data and basin area, mean annual sediment yield and denudation rates for Nanga Parbat are produced. Denudation rates calculated in this fashion range from 0.2 mm year^{-1} in the

---

* Corresponding author. Tel.: +1-916-278-6667; fax: +1-916-278-4650.
E-mail address: cornwell@csus.edu (K. Cornwell).

slower, more sluggish Rupal drainage basin to almost 6 mm year^{-1} in the steeper, faster flowing Raikot and Buldar drainage basins.

1. Introduction

The Nanga Parbat massif is one of the largest topographic features in the western Himalaya of northern Pakistan with its main summit rising to 8126 m and several lesser peaks (Raikot, Chongra, Ganalo, and Mazeno) rising to 7000 m. The massif supports 69 separate glacier systems and produces vertical drops of 7000 m over a 21-km horizontal distance, representing the steepest relief above sea level in the world (Shroder, 1989). The 1250-km^2 massif is drained by nine major rivers that drain the north slope (Patro, Raikot, and Buldar), the east slope (Astore, Goricot, Lotang, and Sachen), the south slope (Rupal), and the west slope (Diamir) (Fig. 1). These rivers (with the exception of the Astore, which generates some of its discharge from terrains beyond the massif) are all fed by high elevation glacial melt waters that produce heavily sediment-laden discharges, and yet sediment production and denudation rates have only been sporadically addressed.

Geologic mapping, petrographic analysis, and cooling-age pattern studies (Zeitler et al., 1993; Schneider et al., 1999a,b; Poage et al., 2000) suggest that the massif has experienced rapid exhumation in the recent geologic past. On the basis of geochronologic evidence, Zeitler et al. (1989) and Winslow et al. (1994) suggested that the entire massif had been exhumed 10 km in the past 10 Ma with 6 km of that exhumation occurring during the last 1.3 Ma. This evidence coupled with the relatively young, high-grade metamorphic and igneous rocks exposed at high elevation (Zeitler et al., 1993) reflects a most rapid rate of uplift and consequent denudation.

Denudation studies in such extreme topography are few. Sediment transport and yield conditions were evaluated for the Raikot glacier on the north slope of Nanga Parbat during the 1980s (Gardner and Jones, 1993), yielding denudation rates of the glacier area of 4.6–6.9 mm year^{-1} and 1.4–2.1 mm year^{-1} for the basin area. Burbank et al. (1996), using exposure ages of incised bedrock surfaces along the Indus River, derived incision rates of 2–12 mm year^{-1} across the Nanga Parbat uplift. Shroder et al. (1999) measured the volume of small debris fans on the south slopes of Nanga Parbat and constrained the timing of their deposition using cosmogenic dating of glacially exposed rocks and sediment to produce denudation rates of about 2 mm year^{-1}. Shroder and Bishop (2000), measuring rates of local incision around the Nanga Parbat massif (15 different localities), determined maximum incision rates for the massif of 22 ± 11 mm year^{-1}.

The significance of denudation rates and processes in high elevation environments is becoming more apparent as science better understands the nature of tectonic uplift, long-term isostatic adjustment, and erosion rates that increase mechanical and chemical weathering processes and likely influence the climatic trends that have fluctuated so dramatically during late Cenozoic time (Raymo et al., 1988; Raymo and Ruddiman, 1992). Substantial chemical weathering (a potentially large sink for atmospheric CO_2) generated from uplift and erosion of vast mountainous areas such as the Himalayas and Tibet may have contributed pronouncedly to the onset of colder climatic conditions.

This paper outlines our efforts to generate conservative estimates of modern-day discharge conditions, measures fluvially stored sediment, calculates sediment transport fluxes, and determines denudation rates from three basins that drain Nanga Parbat. The Raikot (299 km^2) and Buldar (212 km^2) river basins (which drain a portion of the north side of the massif) and the Rupal (315 km^2) River basin (which drains a significant portion of the south side) were chosen for this analysis because of their accessibility and orientation on Nanga Parbat. Approximately 33%, 36%, and 42% of the Raikot, Buldar, and upper Rupal watersheds are glaciated, respectively. Our findings,
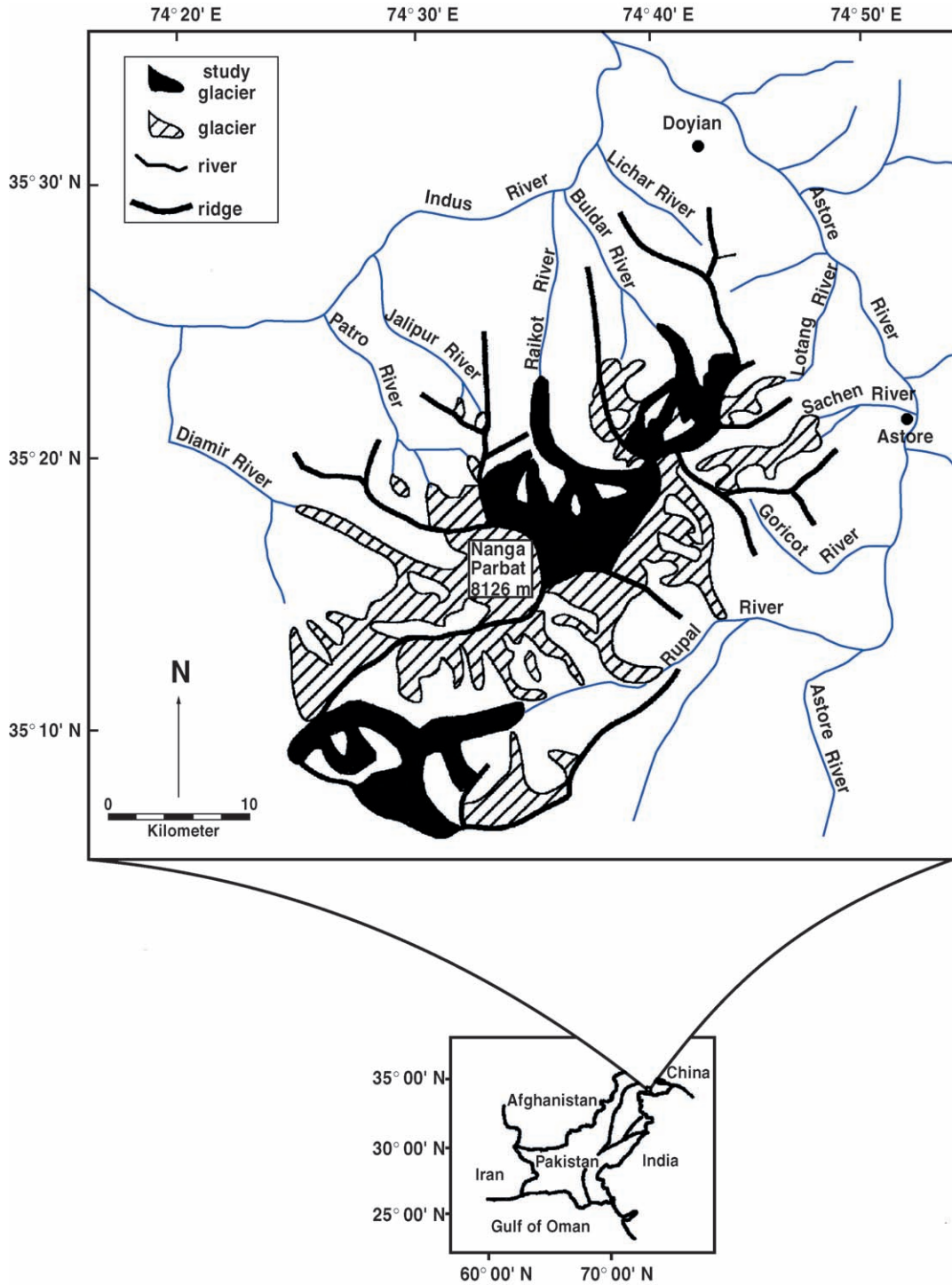
Fig. 1. Location map of Nanga Parbat illustrating the distribution of glacial and drainage networks on the massif.

when combined with comparable glacial and mass wasting estimates, would be expected to illuminate denudation conditions/rates occurring on the Nanga Parbat massif under modern-day climatic conditions and further our growing understanding of denudation rates in such high elevation environments.

2. Fluvial characteristics

Discharges emanating from the high elevation basins included in this study are the result of seasonal monsoon precipitation events and glacial and snow-melt. The annual monsoon storms that impact Nanga Parbat from the south from July through September are the most dominant source of precipitation to the massif. A secondary source of precipitation comes from westerly depressions that are the major source of precipitation during non-monsoonal times (generally the winter months). Young and Hewitt (1990) suggested that the monsoonal influence produces heavy precipitation in basins of Nanga Parbat primarily because of the massif's geographic location in the southern part of the Himalaya Range and its orographic influence on storms tracking to the north. Coupled with the westerly depressions that also produce potentially heavy precipitation in the Himalaya range, the Nanga Parbat massif receives an average of over 1000 mm of precipitation annually (Ali, 1995).

Long-term hydrograph data for the drainage basins of the Nanga Parbat massif is only indirectly available. Fig. 2 illustrates the general features of hydrograph data from the Astore River (drainage area of 4040 km^2) based on sediment transport analysis conducted by the Water and Power Development Authority (WAPDA) in Pakistan during the 1970s and early 1980s at Doyian. Although the sediment yield does not equal discharge, it relates to discharge by proxy. At this station, mean annual flow is 121.0 cm.

The shapes that emerge from this data are characteristics of high elevation drainage basins that are heavily ice and snow covered and experience considerable melting during the warmer summer months. Hydrograph data from the Indus (162,000 km^2), Kabul (67,340 km^2), and Hunza (13,157 km^2) Rivers (Young and Hewitt, 1990) in Fig. 3 show discharge patterns comparable in shape to the Astore River data. Orographic conditions temper monsoonal influences farther north into the Himalaya ranges (characteristic of the Hunza and Kabul drainage systems) suggesting that glacial and snowmelt during the warmer summer season account for substantial volumes of discharge in these river systems.

2.1. Relief ratios

The primary difference observed in the drainage basin relief profiles (Fig. 4) results from incision by
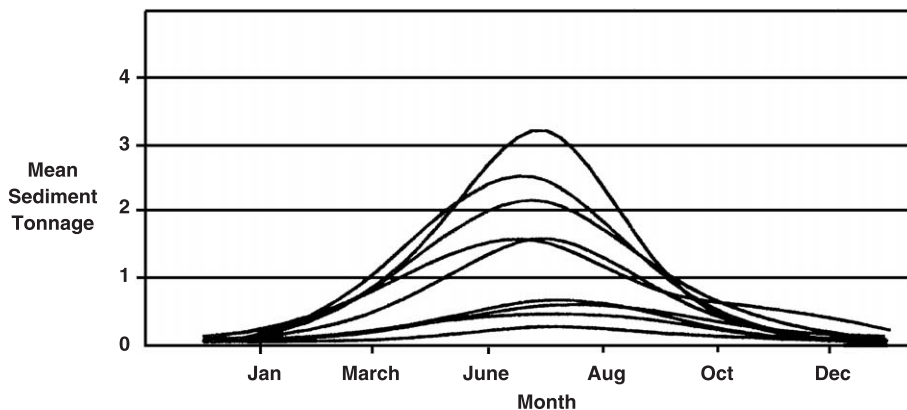
Fig. 2. Sediment yield of the Astore River at the Doyian gage site as measured by the Western Area Power and Development Authority (WAPDA). This data indirectly represents discharge conditions (by proxy) since increased discharges during the summer months correspond to increased sediment yields.
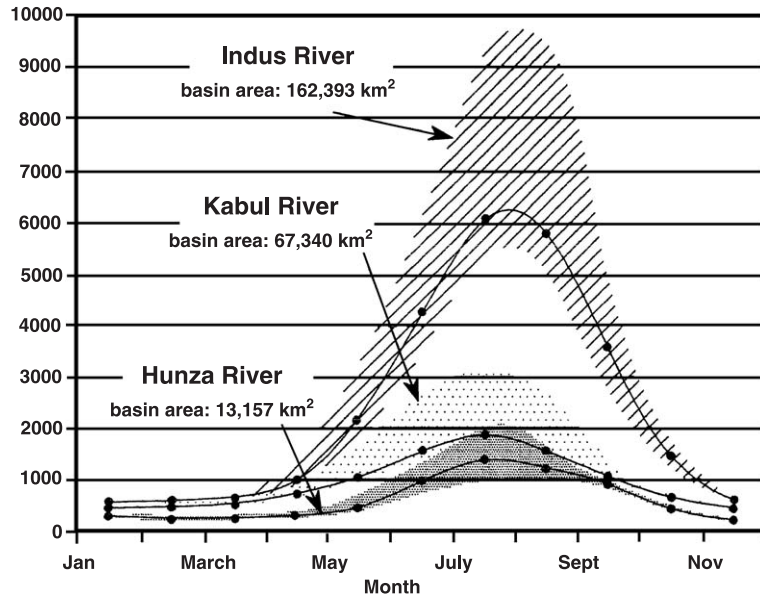
Fig. 3. Hydrograph data from the Indus River (as it drains the Western Himalaya–Besham station) and two of its tributaries, the Kabul River (draining the Hindu Kush Range–Warsak Station) and the Hunza River (draining portions of the Karakoram Range–Dianyor Station) (after Young and Hewitt, 1990).

the Indus River on the north side of the massif. Rapid downcutting of the Indus River over time (Burbank and Beck, 1991; Shroder and Bishop, 2000) has generated a relatively steep slope for north-draining basins (Raikot and Buldar) over a short distance (<15 km), while the Rupal basin experiences comparable elevation changes over a much longer distance (>80 km).

The distance from the glacier terminus and the confluence of the Raikot and Indus Rivers is ~ 13.5 km. Over that distance, the gradient of the channel averages 0.14. About 5.5 km up from the confluence,
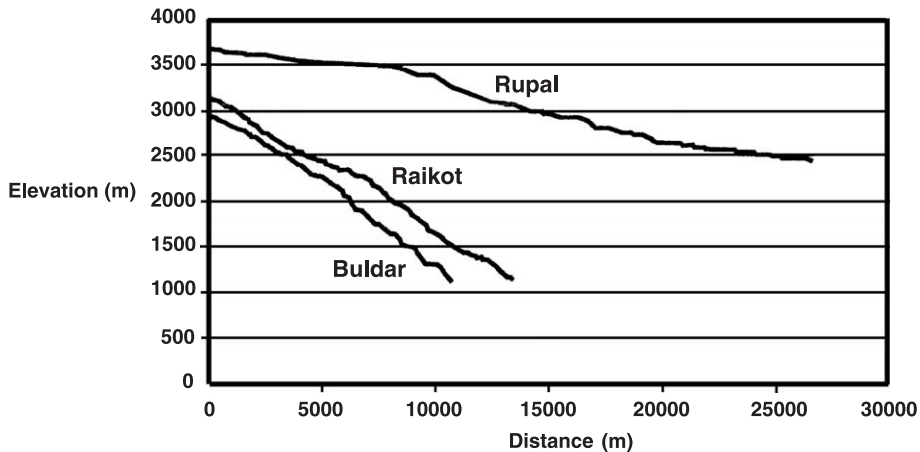

Fig. 4. Drainage basin relief profiles for the Raikot, Buldar, and Rupal valleys.

the slope changes notably and the gradient flattens slightly from 0.16 to 0.11. This condition continues for about 4.5 km farther upstream until the gradient again becomes steeper, reaching a maximum of 0.3 over the remaining 3.5 km to the glacier terminus.

Buldar channel gradient (0.17) is slightly steeper than the Raikot (0.14) and substantially steeper than the Rupal (0.04). The Buldar channel extends ~ 10.7 km from the glacier terminus to the Indus confluence and experiences an elevation change of about 1850 m.

The Rupal River, on the other hand, travels almost 83 km to its confluence with the Indus and produces a much lower gradient of about 0.03. Along the channel stretches included in this study (upper 10 km), the gradient is about 0.04.

Hypsometric analysis of the study basins illustrates the nature of these high elevation, steep gradient valleys (Fig. 5). The Buldar basin has more than half of its mass above its median elevation and represents the steepest gradient within the study basins. The Raikot basin is slightly less than Buldar conditions, while the Rupal basin has a substantial portion of its mass below its median elevation.

2.2. Velocity measurements

We collected velocity measurements at selected localities to generate velocity profiles for comparison and calibration with computer-generated velocity con-ditions. Velocity estimates were calculated by measuring the time of travel of water-filled balloons over a specific distance at various times throughout the day. The 9-in (23-cm) diameter, brightly colored, biodegradable balloons were filled with water (two-thirds capacity) and air (one-third capacity) then released into the middle of the river's flow. When balloons had reached full velocity and were sampling as much of the river flow as possible, timing began.

We realize that this technique does not adequately represent the variability of flow velocity (vertically, laterally, or temporally) in such dynamic settings. Instead, we suggest that this approach generates a rough mean estimate of flow velocity in the primary flow path of the river when measured at the reach-scale. The sometimes-violent nature of flow conditions and access to the active flow channel prohibit utilization of other more accepted means of flow velocity measurements, such as current meters and tracers.

We acknowledge some limitations to this technique, as the balloons generally ride in the upper portion of the flow column (although water-filled balloons are mostly submerged below the surface and sample a more representative flow than objects floating on the surface). Sometimes the balloons get caught in eddies and small discontinuous whirlpools that occasionally eject the balloon out of the water and through the air for short distances. Considering
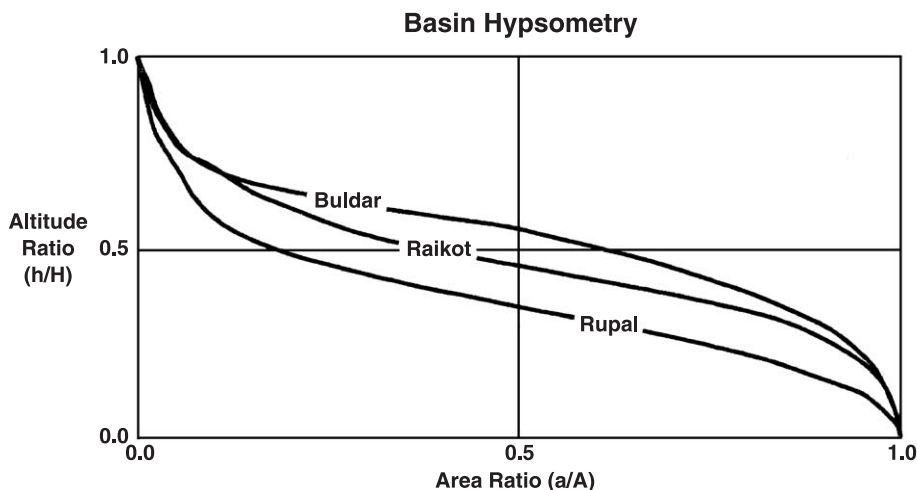

Fig. 5. Hysometric profiles of the Raikot, Buldar, and Rupal valleys through the study reaches.

the turbulent nature of the river system, however, balloon flow data seemed to produce consistent results and errors associated with this approach, which will likely be on the conservative (i.e., lower velocity) side.

The fastest and the slowest times were discarded out of each data set, and the remaining times were averaged to yield mean velocities. Velocity estimates in the Raikot channel varied from a maximum speed of 2.5 m s^{-1} to a minimum of 2.15 m s^{-1} and had a mean value of 2.4 m s^{-1} ± 0.14. Velocity estimates from the Rupal channel varied from a minimum of 1.67 m s^{-1} to a maximum of 2.26 m s^{-1}, with a mean value of 2.13 m s^{-1} ± 0.025.

The lower velocity conditions apparent in the Rupal channel likely are a result of lower gradients (an order of magnitude less than the gradient in the Raikot channel). Considering the level of turbulence in the Raikot River, however, one would expect the velocity to be somewhat inhibited by the general roughness conditions of the channel.

2.3. Discharge estimates

The three basins included in this study (Raikot, Buldar, and Rupal) were all reasonably accessible during the 1996 and 1997 field seasons. Selected channel sections in these basins were surveyed using a laser theodolite to generate cross-sectional data. Fig. 6 outlines the relative location of the study reaches in their respective drainage basins. Channel cross-sectional data were entered into WinXSPRO software (WEST Consultants, 1996) that manages cross-sectional data to generate hydraulic parameters and solve resistance equations to yield velocity, discharge, and shear stress estimates under various stage conditions. The resistance equation selected for this analysis was Jarrett's equation (Jarrett, 1984):

$$n = 0.39 \ S^{0.38} R^{-0.16} \tag{1}$$

where n is Manning's roughness coefficient, S is water surface slope (head loss over a given length of channel), and R is hydraulic radius.

Jarrett's equation yields a value of Manning's n, which is a function of the water surface slope and hydraulic radius at a cross section. Resistance values were then incorporated into solving Manning's equa-

tion to determine mean flow velocity and, consequently, to calculate discharge through each cross section.

Field data indicate that n values are much greater on high-gradient, cobble- and boulder-bed streams than on low-gradient streams having similar relative roughness values (Jarrett, 1987). As gradient increases, energy losses increase as a result of wake turbulence and the formation of localized hydraulic jumps downstream from boulders. With few exceptions, the bank and channel materials were composed of loosely consolidated sediment, ranging in size from predominantly boulders to silts and clays.

2.4. Raikot and Rupal rivers discharge measurements

Inhospitable weather conditions and native peoples in the Buldar valley prohibited direct measurement of discharge conditions in the channel for calibration with WinXSPRO calculations. For these reasons, our discussion of discharge conditions is focused on data collected from the Raikot and Rupal drainage basins.

In two locations along the upper portion of the Raikot River (where conditions allowed), stream depths were probed. The first location was at a small bridge constructed over a relatively narrow (constricted) part of the river about 4 km below the glacier terminus. The flow was too fast and turbulent for probing the depths by hand with a stadia rod from the bridge. Instead, guide ropes were attached to the stadia rod and securely held upstream of the probe point (Fig. 7). This effort allowed the stadia rod to remain relatively straight and not bend or get forced downstream by the river flow. Several probe depths were sounded across the channel at this location and a depth profile was constructed for the channel. The cross-sectional profiles measured in this manner produced area estimates and, when combined with velocity flow measurements, stream discharge. Discharge calculations at the bridge ranged from 29.0 cm at maximum measured flow velocity to 7.6 cm at minimum measured flow velocity.

Depth probes were also conducted near the glacier terminus (about 100 m downstream) where the channel narrows between some large boulders. Velocity data were also obtained through this probe location to evaluate stream discharge. Discharge calculations near the glacier terminus ranged from a maximum dis-
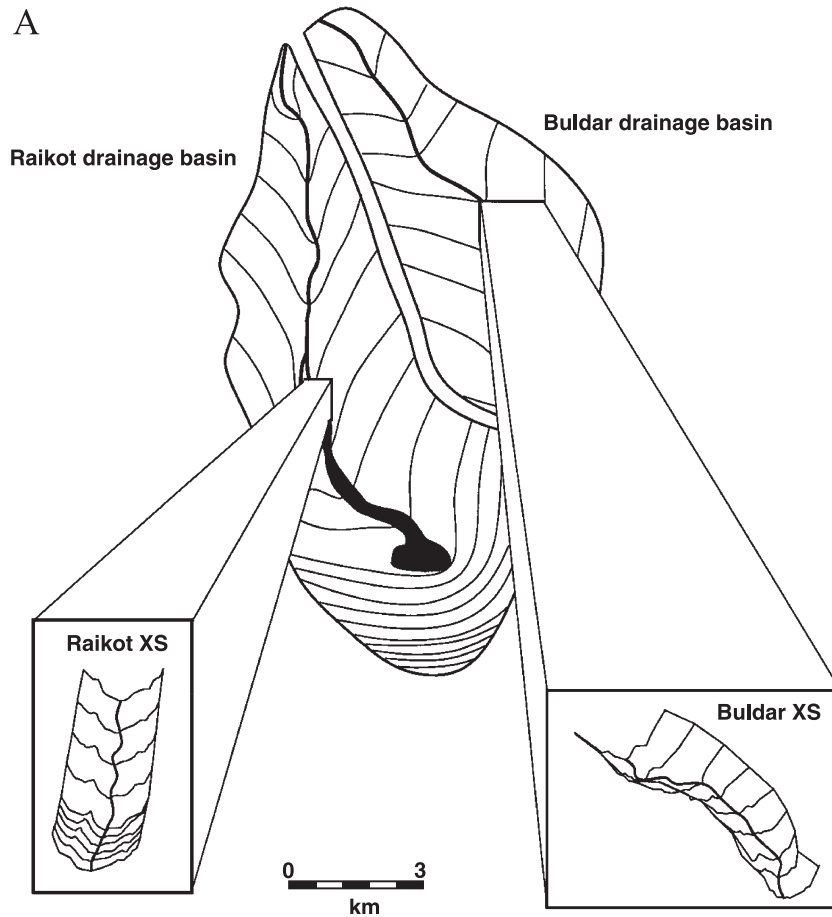
A

Fig. 6. (A) Raikot and Buldar drainage basins and cross sections. (B) Rupal drainage basin and cross sections. See Fig. 1 for basin orientations on Nanga Parbat.

charge of 20.5 (at peak measured flow velocity) to 5.4 cm (at lowest measured flow velocity). The terminus routed most of the flow through the measured section, but 1–2 cm actually flowed around the large boulders that confined most of the flow.

Two locations along the Rupal River were also probed in an effort to determine channel dimensions for discharge estimates. The first locality (just east of the Bazhin Glacier) occurred where a small footbridge crossed the river and offered a straddle point across the 11.3-m-wide channel. The second locality (just west of the Tarshing Glacier) again was chosen because of a footbridge that spanned the 12.6-m-wide channel. Velocity data were obtained through these probe locations to evaluate stream discharge. The

discharge location east of the Bazhin Glacier ranged from a maximum discharge of about 48 cm (at peak velocity) to about 40 cm (at lowest measured velocity). Flow conditions in the Rupal River were much less turbulent than that of the Raikot, likely a function of the much higher channel gradients present in the Raikot basin.

These discharge measurements were compared to equivalent channel areas and discharges calculated using the WinXSPRO software and are summarized in Table 1. The footnoted rows show the equivalent WinXSPRO calculations using Jarrett's equation to ultimately solve for velocity and discharge.

Tables 2 and 3 summarize WinXSPRO calculations for cross sections in the Raikot and Rupal sections
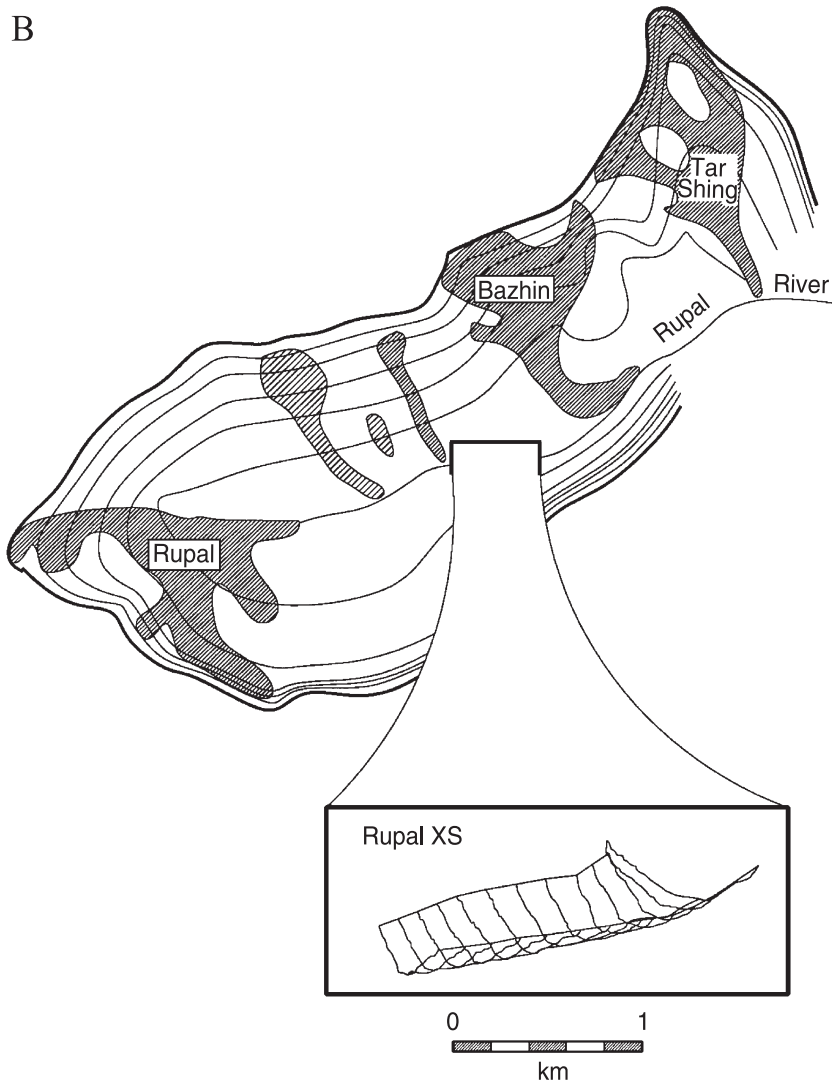
B

Fig. 6 (*continued*).

closest to the field calibration locales. In general, field discharge measurements correlated closely to WinX-SPRO calculations. Subsequent hydraulic estimates and sediment yield calculations are based on discharges generated through WinXSPRO software.

3. Sediment transport characteristics

Sediment transport equations are developed under experimental conditions to determine sensitivities to variable flow and sediment conditions. Thus, it becomes critical that the conditions under which a particular equation was developed are matched in the field study area (Nielson, 1974). Unfortunately, the rivers of the Himalaya in general tend to lie outside the descriptive characteristics under which sediment transport equations tend to be designed.

Gravel transport equations are designed using two primary criteria: discharge and tractive force. Discharge focuses on the quantity of water, cross-sectional area, and slope of a river system, but some

Fig. 7. Probing bedrock conditions and channel cross sections at the Raikot Bridge crossing. Guide ropes were used to stabilize the stadia rod as dynamic flow conditions prohibited direct push approaches.

researchers (McBean and Al-Nassri, 1988) express concern over the confidence of these equations and the practice of determining sediment transport by discharge in general.

Tractive force equations attempt to quantify the shear stress of flowing water on the floor of the channel relative to the channel slope, thereby examining the river–riverbed interface that varies with flow type and bed material properties. Attempts to measure or calculate bed shear stress values in mountain rivers are complicated by the channel bed roughness and the associated turbulence and velocity fluctuations—two variables that are most difficult to quantify.

For this study, the Meyer-Peter and Muller (1948) equation (Nielson, 1974) was chosen for application

Table 1
Channel conditions and discharge calculations for Raikot and Rupal sections

Location	Date	Time	X-sec area (m^2)	Velocity (m s^{-1})	Discharge (ft^3 s^{-1})	Discharge (m^3 s^{-1})
Raikot Bridge (#7)	7/28/97	9:45 am	10.13	2.40	858	24.31
Raikot Bridge (#7)[a]	7/28/97	9:45 am	10.13	2.00	715	20.26
Glacier Portal	8/2/97	11:00 am	7.18	2.50	633	17.95
Rupal Bridge (west) (#11)	8/12/97	9:30 am	22.60	2.13	1700	48.14
Rupal Bridge (west) (#11)[a]	8/12/97	9:30 am	22.60	2.32	1700	52.43
Rupal Bridge (east)	8/14/97	9:25 am	23.68	2.47	2065	58.5
Tarshing Bridge	8/9/97	10:15 am	26.25	2.47	2290	64.84

[a] Discharge calculations using WinXSPRO velocity calculations.

Table 2
Channel conditions and hydraulic calculations for the Raikot survey section nearest the calibration point (cross section #7)

Stage (m)	Area (m^2)	R (m)	Slope	n	VAVG (m s^{-1})	Q (m^3 s^{-1})	Shear (Pa)
0.30	0.75	0.2	0.141	0.201	0.6	0.5	253.8
0.60	2.50	0.3	0.141	0.183	1.0	2.5	454.9
0.90	5.28	0.5	0.141	0.170	1.4	7.5	713.4
1.20	8.50	0.7	0.141	0.162	1.9	15.8	986.3
1.33[a]	10.10	0.8	0.141	0.160	2.0	20.3	1075.0
1.50	12.30	0.9	0.141	0.157	2.2	26.9	1197.0
1.80	16.61	1.1	0.141	0.152	2.6	43.0	1469.9
2.10	21.39	1.2	0.141	0.148	2.9	61.8	1675.8
2.50	28.36	1.5	0.141	0.144	3.4	97.0	2054.1

[a] Comparable stream probing stage height and hydraulic parameters.

primarily because it best accommodated the discharge and sediment conditions present in the rivers of this study. Specifically, the Meyer-Peter and Muller equation uses a tractive force approach that applies to rivers with coarse particle sizes and high gradients. The river systems in this study seem to closely match the experimental conditions used in the generation of the Meyer-Peter and Muller transport equation. Bed load determinations from this solution do not include suspended sediment influences.

Solution of the Meyer-Peter and Muller equation was accomplished using a program that was developed for the U.S. Corps of Engineers by WEST Consultants that characterizes high altitude, steep mountain streams and incorporated flow, and channel characteristics output from WinXSPRO.

Input requirements include the D_{50} particle size of bed particles. Physical measurements of bed load sediments in these river channels were not possible due to the extremely high-energy conditions. Instead, bed load characteristics were evaluated by measuring

sediment sizes along the banks of the river channels and by following the techniques outlined by Wolman (1954) to estimate bed load conditions. Although the measured sediment (100 count) was not in the active portion of the modern channel, their close proximity next to the channel reflected the fact that under higher flow conditions, these sediments were entrained and transported as bed load materials.

3.1. Suspended sediment loads

Raikot River sediment yields were measured throughout a 7-day time period at a location chosen for channel accessibility and where flow conditions were dynamic. Samples were collected at 3-h intervals throughout the day (9:00 a.m., 12:00 a.m., 3:00 p.m., and 6:00 p.m.). In an attempt to further characterize diurnal variations, samples were also collected on an hourly basis between 9:00 a.m. and 6:00 p.m. over a 2-day time period and at 3-h intervals over a 33-h time period.

Table 3
Channel conditions and hydraulic calculations for the Rupal survey section nearest the calibration point (cross section #11)

Stage (m)	Area (m^2)	R (m)	Slope	n	VAVG (m/s)	Q (m^3/s)	Shear (Pa)
0.30	1.03	0.21	0.035	0.115	0.6	0.6	76.6
0.60	2.74	0.40	0.035	0.105	1.0	2.6	134.1
0.90	5.11	0.55	0.035	0.099	1.3	6.5	191.5
1.20	8.14	0.70	0.035	0.095	1.6	12.7	244.2
1.50	11.88	0.88	0.035	0.092	1.9	22.0	296.9
1.80	16.15	1.04	0.035	0.090	2.1	34.3	349.5
2.10	21.23	1.10	0.035	0.089	2.3	48.2	378.3
2.17[a]	22.60	1.14	0.035	0.088	2.3	52.4	391.6
2.50	29.10	1.34	0.035	0.086	2.6	76.8	454.9

[a] Comparable stream probing stage height and hydraulic parameters.

Suspended sediment concentrations were determined using National Water Well Association Method 2540 D (Clesceri et al., 1989). Specifically, a sample 50–100 ml was collected from an active flow portion of the river channel. The sample volume was precisely measured in a graduated cylinder and then slowly pulled by vacuum through a preweighed 45-μm filter. The sediment-laden filter was then dried at ~ 100–105 °F (23.6–26.3 °C) and placed in a desiccator until cooled. The cooled samples were weighed to the nearest 0.001 g and sediment concentrations calculated in units of mg l^{-1}.

The results of these measurements are outlined in Fig. 8. Sediment concentrations ranged from a high of 22,514 mg l^{-1} (7/28/97, 6:00 p.m.) to a low of 562 mg l^{-1} (7/25/97, 6:00 p.m.) with a mean concentration (throwing out the highest and lowest values) of 3970 mg l^{-1} over this time period. Suspended sediment loads calculated from WAPDA data from the Doyian gage site (over a nine year span) yield an annual maximum average suspended concentration of 3480 mg l^{-1}.

The maximum concentrations of sediment in river flow appeared to coincide (as expected) with the afternoon maximum temperature value. As can be seen in Fig. 8, warm afternoons on 7/26, 7/27, and 7/28 resulted in high suspended sediment values, while cloud-covered days/afternoons (7/25, 7/29, 7/30, and 7/31) produced much smaller suspended sediment loads.

We also noticed a direct relationship between the ambient temperatures measured throughout the day and the suspended sediment load. Fig. 8 shows how suspended load concentrations vary as a function of temperature (which affects ice and snow melting and, consequently, discharge volumes).

3.2. Dissolved sediment load

Dissolved solid loads were measured in waters of the Raikot and Buldar Rivers over the course of 7 days, yielding concentrations that ranged from 40 to 60 mg l^{-1} in the Buldar basin and 50 to 105 mg l^{-1} in the Raikot basin. In comparable work in the Absaroka Range in Wyoming, Miller and Drever (1977) determined seasonal variations of the dissolved sediment load. The Absaroka Range is characterized by rocks that are andesitic in composition, rugged

topography (elevation 1760–3700 m), mean annual temperature is 7 °C, and mean annual precipitation is 40–50 cm. The dissolved chemical constituency included K, Cl^-, Mg^+, Ca^+, Na^+, SO_4^{2-}, SiO_2, and HCO_3^- that yielded average dissolved concentrations of 114.2 mg l^{-1} during winter and 71.8 mg l^{-1} in the summer. As is apparent in Miller and Drever's (1977) work, the dissolved load does not appear to vary much through seasons or flow conditions. Considering the water temperature conditions in the river systems draining Nanga Parbat (about 3.5 °C), we would not expect much variation in dissolved capacity as a function of temperature because temperature conditions do not exhibit much variation over time.

In our model of sediment yield, the dissolved sediment load plays a very minor role in sediment contribution. In fact, varying these concentrations by an order of magnitude in either direction does not change the sediment flux noticeably.

3.3. Bed loads

Physical measurement of bed load sediment in the Raikot River channel was not possible because of the extremely high-energy conditions prevalent in the channel. Consequently, bed load concentrations were evaluated by measuring sediment sizes along the banks of the Raikot River channel and by conducting a pebble count analysis (Wolman, 1954). Although the measured sediments were not in the active portion of the modern channel, their close proximity next to the channel indicated that under higher flow conditions, these sediments were entrained and transported as bed load materials.

Pebble count data was incorporated into WinX-SPRO and used to solve the Meyer-Peter and Muller sediment transport equation. This produced bed load rating curves (sediment in tons day^{-1}) as a function of discharge (Fig. 9). The rating curve generated from Raikot data at cross section #7 produced a total sediment load of 11,000 tons day^{-1} (9980 tons day^{-1}) under bank full flow conditions (61 cm). At Rupal cross section #7, rating curve data suggest a total sediment load of 3800 tons day^{-1} (3450 tons day^{-1}) under bank full discharge conditions of 84 cm. Buldar data (cross section #2) produced a total sediment load of 9000 tons day^{-1} (8160 tons day^{-1}) under bank full discharge conditions of 44 cm.

Raikot River Suspended Sediment Concentration and Daily Temperature Records
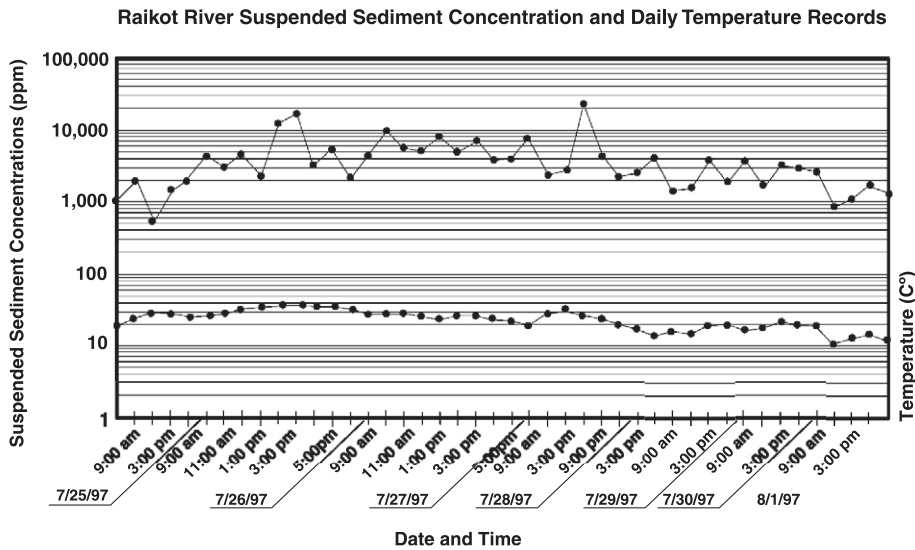
Fig. 8. Suspended sediment loads and temperature data from the Raikot River over the course of 7 days (7/25 – 8/1/97).

It should be noted that the bed load estimates are determined under peak annual discharge conditions, conditions responsible for ~ 88% of the annual load but only occurring over about one-third of the year.

Shear stress components were also calculated (Parker et al., 1982) in WinXSPRO runs as a function of the D_{50} value of the bed load. Shear stresses of about 461 Pa were calculated for bank full discharges in the Rupal River and 1925 Pa at bank full conditions in the Raikot River.

3.4. Sediment storage and residence time

In the glaciated valleys, sediment stored in flood plains filled the parabolic groove left by the passing of earlier glacial events (Harbor and Wheeler, 1992). The
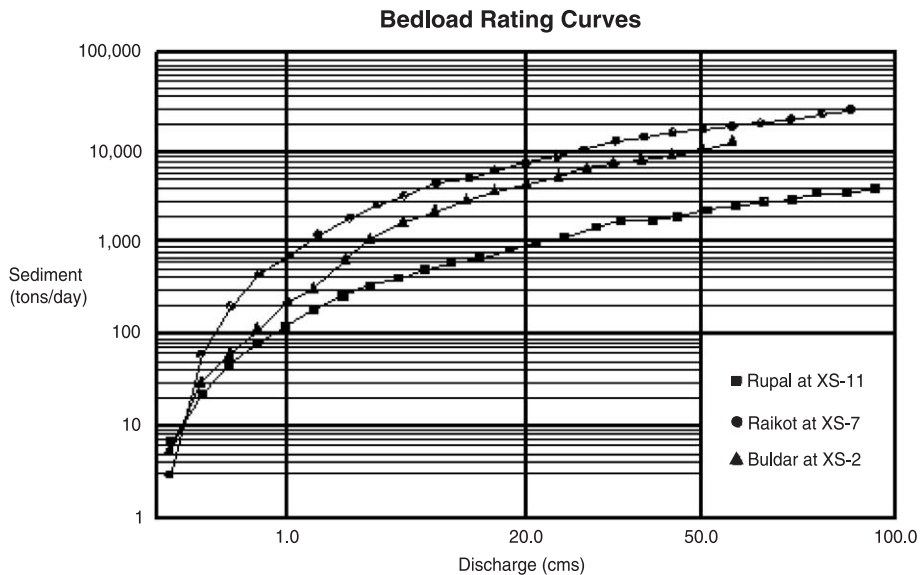
Bedload Rating Curves

Fig. 9. Bed load rating curves for the three study basins calculated from pebble count analysis in WinXSPRO software.
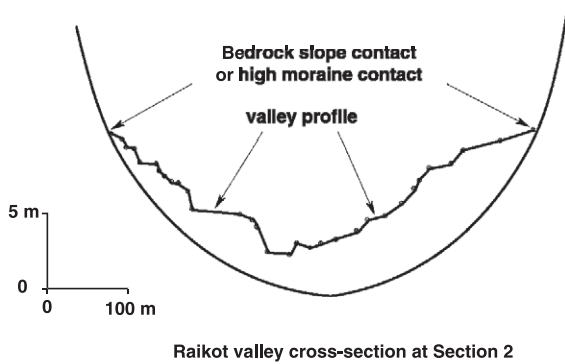
Raikot valley cross-section at Section 2

Fig. 10. Parabolic curve generated through valley cross sections to generate sediment storage estimates.

stored sediment comes from a variety of different sources, including mass wasting, fluvial, glacial, and eolian actions. Once on the valley floor, however, fluvial action becomes the dominant transport process under the modern climatic regime.

The movement of stored sediment in the valleys is dependent on the local hydrologic conditions that vary from month to month and year to year. Rare, high discharge events move substantially more sediment per event than the more frequent lower discharge events,

but they happen so sporadically that most of the work is probably done by the low magnitude, high frequency flow conditions that typify the fluvial regime.

We quantified the total valley fill within the Raikot and Buldar basins by generating a parabolic curve from surveyed elevation profiles of the valley (including high morainal deposits) perpendicular to river flow (Fig. 10). This iterative curve methodology, although not as precise as using bedrock position, is a fair method of quantification, especially in the steep regions of the Himalaya (Harbor and Wheeler, 1992) where valley bedrock data is nonexistent.

Sediment that is not actively being moved down the river is considered to be either temporary (in the active flood plain) or semipermanent (fill that is deeper than the greatest depth of the river within the cross section) stored sediment.

Temporary storage volumes were calculated by constructing riverbank and flood-plain cross sections, multiplying the width of the flood plain by the depth of the river at its deepest point and subtracting the bank full cross-sectional area (Fig. 11).

The sediment below the deepest portion of the riverbed is effectively valley fill that was generated from mass wasting of over-steepened sides of the

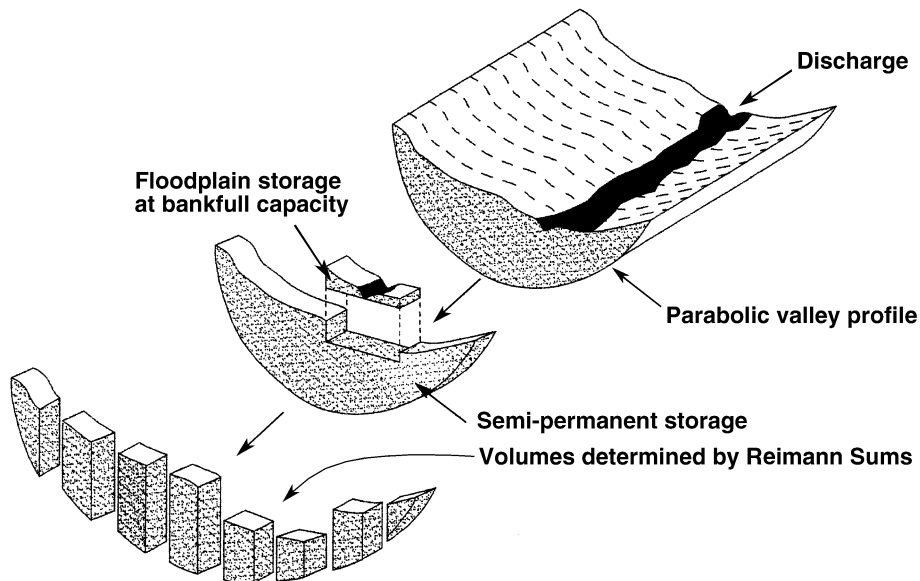## Typical Valley Sediment Storage Conditions

Fig. 11. Sediment storage conditions in the Raikot and Buldar Basins. The Rupal Basin does not share the same geometric shape (tangent glacial valleys and tributaries) as this model outlines and thus could not be accurately quantified with this approach.

Table 4
Sediment storage conditions in the Raikot and Buldar drainage basins and partial conditions in the Rupal basin

Drainage basin	Raikot	Buldar	Rupal
Mean Floodplain storage ($m^3 \, m^{-1}$)	40.7	29.5	64.8
Mean Permanent storage ($m^3 \, m^{-1}$)	1.97×10^6	2.32×10^6	n/a
Valley length-glacier terminus-outlet (km)	13.2	11.9	7.2[a]
Total Floodplain storage (m^3)	537,240	351,050	466,560
Total valley storage (m^3)	2.6×10^{11}	2.8×10^{11}	n/a
Mean annual sediment yield ($m^3 \, year^{-1}$)	1.682×10^6	5.55×10^5	1.36×10^5
Residence time (h)	17.6	57.6	252.4

n/a—not applicable.

[a] Valley length in upper watershed only (not to outlet).

glacially carved valley. In these areas, more sediment is added to the valley than can be effectively removed by fluvial action. Thus, within a cross section, an overall increase over time of the elevation of the riverbed can be expected. This condition would persist until larger-scale climatic conditions reactivate these valley fill sediments.

Once an acceptable parabolic fit was obtained, Reimann sums were used to estimate the total valley fill. Table 4 outlines the volume of sediment in the various storage reservoirs calculated for the Raikot, Rupal, and Buldar basins. The geographic nature of the Rupal valley (receives drainage and sediment from adjoining ranges that are not part of Nanga Parbat) does not lend itself to quantifying its sediment storage capabilities to the Indus River outlet, so those values are only calculated throughout the upper watershed and not extrapolated throughout the entire valley. All subsequent erosion and denudation values reported for the Rupal valley are reported for the upper-most section of the valley only and should not be extrapolated to the entire Rupal valley.

3.5. Sediment yield

No flow duration data was available on or in close proximity to the Nanga Parbat massif. A 9-year record of sediment yield (suspended only) has been established by WAPDA at the Doyian station along the Astore River. The drainage area of the Astore River at Doyian is 4040 km^2, producing a mean discharge

(over this 9-year record) of about $3.75 \times 10^9 \, m^3$ $year^{-1}$. The WAPDA data indicates that 88% ($\pm 7\%$) of the sediment that is transported in a calendar year (and by proxy, discharge) occurs during the monsoonal months of June through September. Actual sediment yield data show variations in percentages ranging from 96% to 76%.

We calculated the bank full discharge capacity at Raikot, Buldar, and Rupal River cross sections and considered these discharges to account for 88% of the annual discharge and sediment yield generated throughout a calendar year. The remaining 12% of flow and sediment yield is expected to occur during the remaining calendar months (October through May).

Sediment transport fluxes were found for bank full stage conditions for selected cross sections in the study river systems. Selected cross-sections were chosen based on our ability to accurately determine depth of the channel from field surveys. We calculated the mean discharge during the monsoonal season and the non-monsoonal season (discharge values changed markedly) and multiplied that by the sediment transport rate (produced from the U.S. Army Corps of Engineers software) to produce an annual sediment load (Table 5). We then extrapolated that annual load across the area of the drainage basin and determined the maximum and minimum rate of denudation for the respective basins (Table 6).

The denudation rates we calculated for the Rupal drainage basin are consistent with those calculated from volumetric estimates of debris fans over time ($\sim 2 \, mm \, year^{-1}$ from Shroder et al., 1999) on the south slopes of Nanga Parbat massif (remember that the Rupal values only reflect the upper-most section of the entire Rupal drainage network). Denudation

Table 5
Data used to calculate annual sediment loads in the study drainage basins

River section	Bank full stage (m)	Bank full discharge ($m^3 \, s^{-1}$)	Sediment load/ monsoonal season (88%) ($m^3 \, year^{-1}$)	Annual sediment load ($m^3 \, year^{-1}$)
Raikot 1	2.2	28.9	4.32×10^5	4.91×10^5
Raikot 3	2.4	60.5	1.480×10^6	1.682×10^6
Buldar 4	1.2	15.8	1.15×10^5	1.31×10^5
Buldar 2	1.7	43.8	4.89×10^5	5.55×10^5
Rupal 11	2.2	61.8	5.47×10^4	6.22×10^4
Rupal 7	2.3	84.4	1.19×10^5	1.36×10^5

Table 6
Denudation rates for drainage basins in the study

	Rupal		Raikot		Buldar	
Drainage basin area (km^2)	315		299		212	
	Min	Max	Min	Max	Min	Max
Sediment load (m^3 year^{-1})	6.2×10^4	1.4×10^5	4.9×10^5	1.7×10^6	1.3×10^5	5.6×10^5
Denudation (mm year^{-1})	0.2	0.4	1.6	5.6	0.6	2.6

rates from the steeper north slope of Nanga Parbat also are comparable with previous efforts (Gardner and Jones, 1993), which yielded basin-wide estimates of 1.4–2.1 mm year^{-1} in the Raikot basin.

4. Floods

In addition to the continual, gradual fluvial removal of sediment, high magnitude, low frequency flooding events occur sporadically on the Nanga Parbat massif. Two supraglacial floods from the Shaigiri Glacier in the Rupal Valley have redistributed ∼ 6000 m^3 worth of sediment within the drainage basin (much of it being washed out into larger drainage networks off the Nanga Parbat massif) over the last 10 years. During non-flood years, supraglacial meltwaters have only contributed about 100 m^3 of sediment to the transport budget.

The Rupal Valley, with its many glacier-fed tributaries, shows much evidence of the frequency of such events with shorelines of temporary lakes (resulting from glacially blocked and ponded rivers), high discharge scour channels, fields of flood-deposited boulders, and pendant bar deposits (Shroder et al., 1998).

The Tarshing Glacier blocked the Rupal River in 1851 and again in 1856, producing lakes about 2.2 km long and 65 m deep before rupturing the glacier terminus and catastrophically discharging. Water volumes of 16×10^6 m^3 drained for up to 3 days causing considerable erosion of the channel system.

Raikot Glacier has also produced flood events. During the winter of 1994, the subglacial drainage system of the glacier was blocked about 1.5 km upstream from the glacial terminus for several months. Breakout thresholds were breached and more than 45,000 m^3 of sediment from the side and frontal areas

of the glacier were removed. Approximately 19,000 m^3 of these sediments were redeposited along the drainage way, while the rest were carried downriver.

We recognize the significance of these low frequency, high magnitude events and their ability to move large quantities of sediment from the high elevation basins outlined in this study. The inconsistent nature of such events and an inability to temporally characterize their contribution has led us to recognize their occurrence but not include their sediment transport capabilities in our calculations. The addition of periodic flood-transported sediments would be expected to increase the denudation rates calculated herein.

5. Conclusions

We calculated modern denudation rates on Nanga Parbat that ranged from < 1 mm year^{-1} in the more sluggish, lower energy upper Rupal drainage basin that drains the south slope of the massif to almost 6 mm year^{-1} in the more energetic Raikot, and Buldar drainage networks that drain portions of the north slope. The relatively steep slopes associated with the Raikot and the Buldar basins generate greater shear stresses, more turbulent flow, and transport more sediment than the more gently sloping Rupal reach.

These values are consistent with denudation rates on the massif calculated using other methods such as debris fan accumulation rates (Shroder et al., 1999; ∼ 2 mm year^{-1} over the last 5000 year), sediment yield from the Raikot Glacier (Gardner and Jones, 1993; ∼ 4.6–6.9 mm year^{-1} for the glacier area and 1.4–2.1 mm year^{-1} for the basin area), and the dissection and incision of glacially deposited high terrace by fluvially processes (Shroder and Bishop, 2000; ∼ 22 ± 11 mm year^{-1}). In nearby work along

the Indus, Burbank et al. (1996) determined bedrock incision rates to vary from 2 to 12 mm year^{-1}. More regionally based studies (Hewitt, 1972; Ferguson, 1984; Hallet et al., 1996) suggested that denudation rates of more than 1 mm year^{-1} are not unusual in such dynamic settings.

On a broader scale, summary work by Hallet et al. (1996) showed much higher denudation rates (termed effective erosion rates) of 20.31 mm year^{-1} (unweighted average) occurring in glaciated drainage basins in SE Alaska where long-term (>10 year in length) records exist. In general, these glacial systems are fast moving and often much larger in area (many

hundreds to thousands of square kilometers in area) than the basins studied on Nanga Parbat. The effective erosion rate reported is primarily a function of glacial erosion, debris entrainment, and fluvial transport. Long-term effective erosion rates >47 mm year^{-1} (Cai, 1994) have been reported in drainage basins in SE Alaska that are comparable in area to the basins outlined in this study. Short-term records (<10 year in length) of other glaciers in SE Alaska yielded unweighted averages of 30.39 mm year^{-1}, with some rates exceeding 60 mm year^{-1} (Hunter, 1994). Fig. 12 shows how the denudation rates and sediment yield quantities determined in this study compared to other
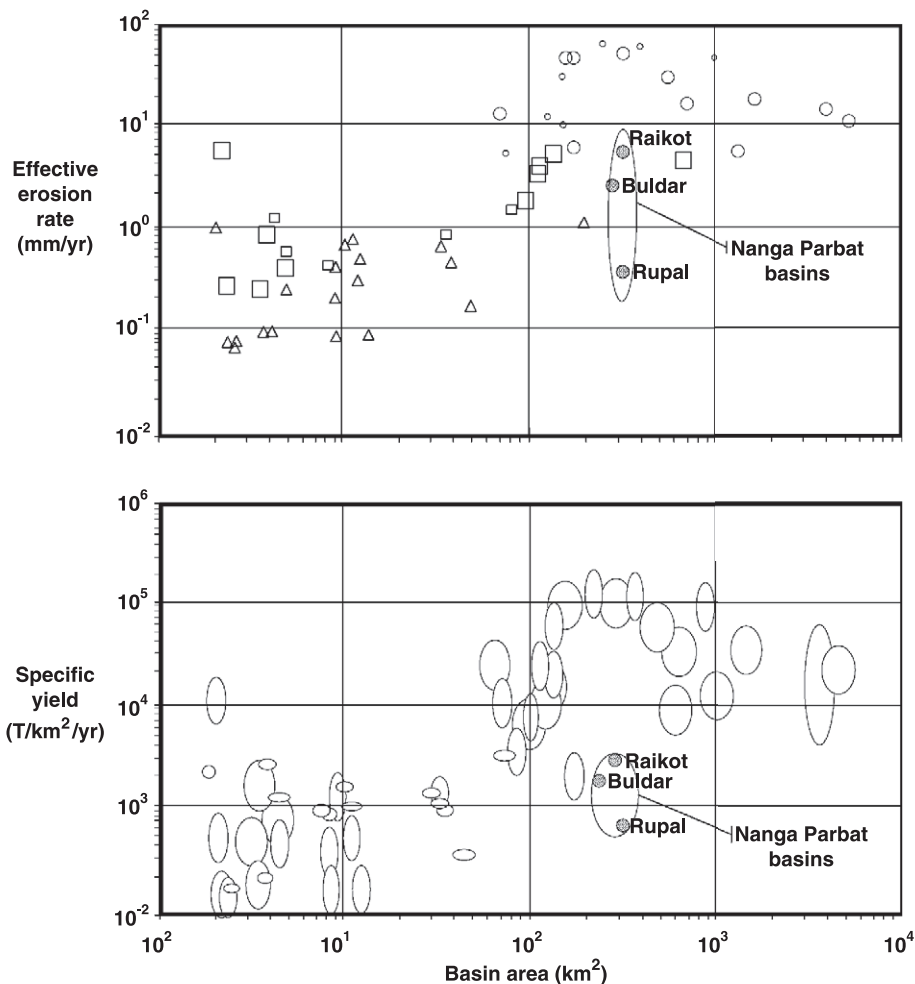

Fig. 12. Global perspective of Nanga Parbat denudation rates and sediment yield conditions as compared to other glaciated mountain systems (after Hallet et al., 1996). Circles refer to glaciers from SE Alaska, small squares to the Swiss Alps, triangles to Norway/Svalbard, and squares to other regions including New Zealand, Asia, and Iceland.

glacial drainage basins compiled in Hallet et al. (1996). Specific yield conditions and denudation rates (reported as effective erosion rate by Hallet et al., 1996) calculated for the basins on Nanga Parbat rank within the general trend of central Asian glaciers included in Hallet et al.'s (1996) compilation. Most of the yield data from comparable basin areas in Fig. 12 come from drainage basins in SE Alaska that receive significantly more precipitation (building larger glaciers) and consequently does more erosional work (both producing and transporting sediment) than the drainage basins on Nanga Parbat, perhaps accounting for the more prolific yield conditions and erosion rates.

The denudation rates derived herein fall on the low side of our initial calculations. Considering the steep relief and the energetic glacial systems on NP, we anticipated higher denudation rates. Several reasons may account for the discrepancy, all of which are related to the difficulty of collecting accurate, precise, and reliable flow and sediment data at Nanga Parbat. First, our field data represent conditions during a short time frame during low flow conditions. Collecting sediment load data over an entire melt season would generate a more complete picture of the fluxes inherent in such a dynamic system and would allow for more comprehensive modeling of erosion rates. Longer sampling intervals would offer even more comprehensive insights. Second, we have not attempted to model extreme events such as subglacial outburst floods and heavy melt/high precipitation events that would generate substantial discharge and sediment yields. Third, bed load probably accounts for a greater proportion of the total sediment load in extraordinary steep mountain stream than in other environments, but an independent source of bed load data does not exist against which we could evaluate our estimates.

Clearly, one of the challenges to developing quantitative understandings of high-elevation fluvial systems and subsequent denudation rates is the general paucity of discharge data available from such sites. Consequently, indirect methods are commonly employed to estimate discharge conditions. These methods, however, often assume steady, uniform flow conditions (conditions that are rare in such dynamic systems), leading often to inaccurate discharge determinations (Jarrett, 1987). Coupled with this limitation with the overall dynamic and variable nature of surficial processes over time, the task seems overwhelmingly complex indeed. This complexity has been most ably described by Shroder and Bishop (2000) who state that "the overall denudation of the Nanga Parbat massif is a spatially and temporally complex mosaic of topography produced by tectonics overprinted with the surficial processes of mass movement, glaciers, rivers and catastrophic floods, all operating at different rates, through time".

Acknowledgements

References

Ali, M., 1995. The Northern Area of Pakistan, Physical and Human Geography. Survey of Pakistan, Pakistan.

Burbank, D.W., Beck, R.A., 1991. Models of aggradation versus progradation in the Himalayan foreland. Geologische Rundschau 80 (3), 623–638.

Burbank, D.W., Leland, J., Fielding, E., Anderson, R.S., Brozovic, N., Reid, M.R., Duncan, C., 1996. Bedrock incision, rock uplift and threshold hillslopes in the northwestern Himalayas. Nature 379, 505–510.

Cai, J., 1994. Sediment yields, lithofacies architecture and mudrock characteristics in glaciomarine environments. PhD dissertation, Northern Illinois University, Dekalb.

Clesceri, L.S., Greenberg, A.E., Trussell, R.R. (Eds.), 1989. Standard Methods for the Examination of Water and Wastewater, 17th ed. National Water Well Association Method 2540 D. National Water Well Association. American Public Health Association, pp. 2-71 to 2-77.

Ferguson, R.I., 1984. Sediment load of the Hunza River. In: Miller, K.J. (Ed.), The International Karakoram Project, vol. 2. Cambridge Univ. Press, Cambridge, UK, pp. 581–598.

Gardner, J.S., Jones, N.K., 1993. Sediment transport and yield at the Raikot Glacier, Nanga Parbat, Punjab Himalaya. In: Shroder Jr., J.F., (Ed.), Himalaya to the Sea. Geology, Geomorphology, and the Quaternary. Routledge, London, England, pp. 184–197.

Hallet, B., Hunter, L., Bogen, J., 1996. Rates of erosion and sediment evacuation by glaciers: a review of field data and their implications. Global and Planetary Change 12, 213–235.

Harbor, J.M., Wheeler, D.A., 1992. On the mathematical descrip-

tion of glaciated valley cross-sections. Earth Surface Processes and Landforms 17, 477–485.

Hewitt, K., 1972. The mountain environment and geomorphic processes. In: Slaymaker, H.O., McPherson, H.J. (Eds.), Mountain Geomorphology: Geomorphological Processes in the Canadian Cordillera. Tantalus Research, Vancouver, British Columbia, No. 14, 17–34.

Hunter, L.E., 1994. Ground-line systems of modern temperate glaciers and their effects on glacier stability. PhD dissertation, Department of Geology, Northern Illinois University, Dekalb, 467 pp.

Jarrett, R.D., 1984. Hydraulics of high-gradient streams. American Society of Civil Engineers, Journal of Hydraulics Division 110 (HY11), 1519–1539.

Jarrett, R.D., 1987. Errors in slope-area computations of peak discharges in mountain streams. Journal of Hydrology 96, 53–67.

McBean, E.A., Al-Nassri, S., 1988. Uncertainty in suspended sediment transport curves. Journal of Hydraulic Engineering 114 (1), 257–264.

Meyer-Peter, E., Muller, R., 1948. Formulas for bed load transport. In: Report on Second Meeting of the International Association of Hydraulic Structures Research, Stockholm, Sweden, pp. 373–410.

Miller, W.R., Drever, J.I., 1977. Chemical weathering and related controls on surface water chemistry in the Absaroka Mountains, Wyoming. Geochimica et cosmochimica acta 41, 1693–1702.

Nielson, D.R., 1974. Sediment transport through high mountain streams of the Idaho Batholith. MS thesis, University of Idaho, Moscow, pp. 6–12.

Parker, G., Klingeman, P., McLean, D., 1982. Bedload and size distribution in paved gravel-bed streams. Journal of the Hydraulics Division 108(HY4) (198204), 544–571.

Poage, M.A., Chamberlain, C.P., Craw, D., 2000. Massif-wide metamorphism and fluid evolution at Nanga Parbat, northwestern Pakistan. American Journal of Science 300, 463–482.

Raymo, M.E., Ruddiman, W.F., 1992. Tectonic forcing of late Cenozoic climate. Nature 359, 117–122.

Raymo, M.E., Ruddiman, W.F., Froelich, P.N., 1988. Influence of late Cenozoic mountain building on ocean geochemical cycles. Geology 16, 649–653.

Schneider, D.A., Edwards, M.A., Kidd, W.S.F., Khan, M.A., Seeber, L., Zeitler, P.K., 1999a. Tectonics of Nanga Parbat, western Himalaya: synkinematic plutonism within the doubly vergent shear zones of a crustal-scale pop-up structure. Geology 27, 999–1002.

Schneider, D.A., Edwards, M.A., Kidd, W.S.F., Zeitler, P.K., Coath, C., 1999b. Early Miocene anatexis identified in the western syntaxis, Pakistan Himalaya. Earth and Planetary Science Letters 167, 121–129.

Shroder, J.F., 1989. Hazards of the Himalayas. American Scientist 77, 564–573.

Shroder Jr., J.F., Bishop, M.P., 2000. Unroofing of the Nanga Parbat Himalaya. In: Khan, M.A., Treloar, P.J., Searle, M.P., Jan, M.Q. (Eds.), Tectonics of the Nanga Parbat Syntaxis, the Western Himalaya. Geological Society of London Special Publication, vol. 170, pp. 163–179. London.

Shroder Jr., J.F., Bishop, M.P., Scheppy, R. 1998. Catastrophic flood flushing of sediment, western Himalaya, Pakistan. In: Kalvoda, J., Rosenfeld, C.L. (Eds.), Geomorphological Hazards in High Mountain Areas. Kluwer Acad. Pub., pp. 27–48.

Shroder Jr., J.F., Scheppy, R.A., Bishop, M.P., Denudation of small alpine basins, Nanga Parbat Himalaya, Pakistan. Arctic, Antarctic, and Alpine Research 31, 121–127.

WEST Consultants, 1996. WinXSPRO: A Channel Cross-Section Analyzer. WEST Consultants, Carlsbad, CA.

Winslow, D.M., Zeitler, P.K., Chamberlain, C.P., Hollister, L.S., 1994. Direct evidence for a steep geotherm under conditions of rapid denudation, Western Himalaya, Pakistan. Geology 22, 1075–1078.

Wolman, M.G., 1954. A method of sampling coarse river-bed material. American Geophysical Union Transactions 35 (6), 951–956.

Young, G.J., Hewitt, K., 1990. Hydrology research in the upper Indus basin, Karakorum Himalaya, Pakistan. In: Molnar, L. (Ed.), Hydrology of Mountainous Areas. IAHS Publ., vol. 190. Wallingford, UK, pp. 139–152.

Zeitler, P.K., Sutter, J.F., Williams, I.S., Zartman, R., Tahirkheli, R.A.K., 1989. Geochronology and temperature history of the Nanga Parbat-Haramosh massif, Pakistan. In: Malinconico, L.L., Lillie, R.J. (Eds.), Tectonics of the Western Himalaya. Geological Society of America Special Paper, vol. 232. Boulder, CO, pp. 1–22.

Zeitler, P.K., Chamberlain, C.P., Smith, H.A., 1993. Synchronous anatexis, metamorphism, and rapid denudation at Nanga Parbat, Pakistan Himalaya. Geology 21, 347–350.